RSC Advances

ROYAL SOCIETY OF CHEMISTRY

www.rsc.org/advances

Regeneration of Dentin-pulp-like Tissue Using Injectable Tissue Engineering Technique

Linhua Tan[1,3], Jun Wang[4], Shuo Yin[3], Wenting Zhu[4], Guangdong Zhou[1,3], Yilin Cao[1,3]*, Lian Cen[1,2,3]*

[1]Department of Plastic and Reconstructive Surgery, Shanghai 9th People;s Hospital, Shanghai Jiao Tong University School of Medicine. No.639 Zhi Zao Ju Road, Shanghai, 200011, China.

[2]Shanghai Key Laboratory of Multiphase Materials Chemical Engineering, Department of Product Engineering, School of Chemical Engineering, East China University of Science and Technology. No.130 Mei Long Road, Shanghai, China, 200237.

[3]National Tissue Engineering Center of China, No.68 East Jiang Chuan Road, Shanghai, China, 200241.

[4]Department of Pediatric Dentistry, School of Stomatology, Ninth People;s Hospital, Medical College, Shanghai Jiaotong University, No.639 Zhi Zao Ju Road, Shanghai, 200011, China;

Running title: Injectable tissue engineering technique to regenerate dentin-pulp complex

* To whom correspondence should be addressed.

Tel: +86-21-64252808; Fax: +86-21-64253159.

E-mail: Dr. Lian Cen: cenlian@hotmail.com

Dr. Yilin Cao: yilincao@yahoo.com

Abstract

An injectable tissue engineering method was developed for dentin-pulp complex regeneration using an injectable scaffold, crosslinked hyaluronic acid gel (HAG). A cell-scaffold composite composed of HAG, tooth buds-derived dental mesenchymal cells (DMCs), and transforming growth factor-β1 (TGF-β1) was prepared and injected subcutaneously in nude mice. Moreover, β-tricalcium phosphate (β-TCP) and polyglycolic acid (PGA) were respectively chosen as control scaffolds for dentin-pulp regeneration. The suitability of injectable HAG for dentin-pulp complex engineering was further demonstrated in empty tooth slices and pulp chamber of mini pigs. Histological and immunohistochemical staining was carried out to identify the distinctive tubular dentin and pulp structure, which was further confirmed by the detection of several dentinogenesis related genes, *DSPP*, *DMP-1*, *MEPE*, and *BSP*. It was found that a recognizable dentin-pulp like tissue with typical well organized dentinal tubular structure, columnar odontoblast-like cells was successfully engineered using the injectable HAG scaffold within the subcutaneously area of nude mice according to histological staining. High expression of genes, *DSPP, DMP-1, MEPE* and *BSP*, in the above neo-tissue as well as positive immunohistochemical staining for dentin sialoprotein (DSP) confirmed the dentinal characteristics. No typical dentin or pulp-like tissue was formed when PGA or β-TCP were used as scaffolds. The efficacy of such method was further demonstrated in empty tooth slices and pulp chambers of mini pigs which had been pre-treated by removal of total pulp and partial dentin. Through the successful delivery of DMCs and TGF-β1 by injectable HAG scaffold, the destroyed dentin was vividly repaired along with the formation of pulp-like tissue. Hence, the current strategy to engineer dentin-pulp complex can overcome the difficulty of specific anatomical arrangement of pulp and dentin with minimal invasion, finally leading to their regain of vitality which is difficult to realize by the current clinical treatments.

Keywords: injectable; dentin-pulp; regeneration; hyaluronic acid gel; dentin sialoprotein

Introduction

Injuries, such as trauma, deep cavity preparation or severe caries, can possibly lead the pulp to irreversible pulpitis or necrosis. Generally, conventional clinical treatment protocol known as root canal or endodontic therapy is indicated in such situations,[1, 2] in which the entire pulp is amputated by pulpectomy and the pulp space is then disinfected and replaced with a rubber-like material "gutta percha".[2] However, in spite of the reported clinical success, the endodontically-treated teeth become devitalized, brittle and susceptible to postoperative fracture or other complications. The loss of pulp vitality in young permanent teeth terminates dentine formation and subsequent tooth maturation.[3] Furthermore, pulpless teeth have lost defensive ability and have no sensation to irritations, resulting in caries progression unnoticed by patients and the subsequent extraction of the teeth. Long-term studies have revealed that tooth loss is higher for endodontically treated teeth than non-treated because of secondary caries and complex restoration associated problems.[2, 4] Therefore, it is of great importance to regenerate functional dentin-pulp complex to replace the lost pulp and dentin, in which situation the decayed tooth may possibly escape the fate of extraction.

Along with the boom and widely usage of tissue engineering technology, it seems that it could provide an attractive strategy for dentin and pulp regeneration.[5-10] However, it is thought to be a tough challenge to regenerate the entire pulp and dentin in situ due to the anatomical arrangement of pulp chamber, which is encased within dentin and mainly relies on one apical foramen to allow angiogenesis for the engineered tissue.[1, 2, 11] Hence, in order to realize the clinical translation of relevant pulp regeneration, rigid scaffold is not a good choice, constrained by the inherent character that they can't penetrate and adapt to the dentin walls throughout the entire root canal. Moreover, pulp is a type of soft tissue while its surrounding dentin is relatively hard. Dentin-pulp complex is a structure containing both hard and soft tissues. Generally, scaffolds often used for soft tissue regeneration, such as polyglycolic acid (PGA) and collagen, were difficult for hard tissue engineering,

whereas scaffolds such as β-tricalcium phosphate (β-TCP) and bioceramics, were mainly used for hard tissue regeneration, e.g. bone.[9, 12-17] Therefore, it is of great necessity to develop a suitable and injectable scaffold which can penetrate the entire root canal space[1, 4, 5, 8, 18-22] and is also easy for clinical application. Hyaluronic acid (HA) glycosaminoglycans present in the extracellular matrix of dental pulp is important in maintaining morphologic organization by preserving extracellular spaces. It also contributes to the initial development of dental pulp and dentin.[4, 23, 24] As is known, HA is biocompatible, biodegradable, bioactive, non-immunogenic and non-thrombogenic.[25, 26] Additionally, HA and its derivatives have been clinically used as medical products for over three decades.[27] HA based gels are usually prepared by cross-linking via different kinds of cross-linkers. 1,4-butanediol diglycidyl ether (BDDE) is one of those commonly used crosslinkers. It has a significantly lower toxicity than other ether-bond crosslinking chemistry based agents. Moreover, it is used in the majority of the market-leading HA fillers. The long safety record of BDDE crosslinked HA gels had spanned more than 15 years, which makes it as an industry standard, ahead of other crosslinkers such as divinyl sulfone and 2,7,8-diepoxyoctane.[28] Hence, BDDE cross-linked HA gels (HAG) in the form of microparticles were proposed to be used as an injectable scaffold to regenerate dentin-pulp complex in this work. Tooth buds-derived dental mesenchymal cells (DMCs) were used as seed cells to be combined with HAG since DMCs can differentiate into dentin-secreting odontoblasts and were previously used as seed cells for dentin-pulp complex regeneration based on tooth developmental theory[2, 29-36].

In this work, HAG, utilized as an injectable scaffold, was combined with DMCs to form a cell-scaffold composite which was then transplanted subcutaneously into nude mice to regenerate dentin-pulp like tissue. Within the above cell-scaffold composite, transforming growth factor-β1 (TGF-β1) was supplemented as it stimulates matrix secretion, initiates odontoblast cytodifferentiation in vitro and in vivo, and is also essential for the homeostasis of the dentin-pulp complex.[37, 38] The duration of in vivo construction was also varied to investigate the influence of time on the regenerated tissue. Moreover, β-TCP and PGA were respectively chosen as control

scaffolds as they were typical scaffolds for hard and soft tissue regeneration. The neo-regenerated tissues constructed from the above three scaffolds were compared macroscopically and microscopically. The suitability of the injectable HAG for dentin-pulp complex engineering was further demonstrated even in empty tooth slices and pulp chamber of mini pigs.

Materials and Methods

Culturing of porcine DMCs

The surgical procedures were permitted by the Animal Care and Experimental Committee of Shanghai Jiao Tong University, School of Medicine. Tooth buds were isolated from jaws of newly born porcine and washed with 0.25% chloramphenicol solution for 3 times. The tooth bud tissue was then minced into < 2 mm^3 pieces, and enzymatically treated with 0.15% collagenase (NB4 Standard Grade, SERVA) and 0.5U/ml dispase II (Neutral protease, Roche) in DMEM/F12(1:1) (HyClone) with 15% fetal bovine serum (FBS) (HyClone) for 1.5 h at 37°C. After that, the digested tooth bud tissues were strained with nylon filter (100-μm pores) and the harvested primary individual dental bud cells were cultured with DMEM/F12 (1:1) with 15% FBS and antibiotic/antimycotic solution (300/ml penicillin G, 300μg/ml streptomycin, 0.75μg/ml amphotericin B) (HyClone) at an incubator at 37°C with 5% CO_2.[39] These cells were cultured for 5~7 days before reaching confluence and they formed a mixed population of epithelial- and fibroblast-like cells. The cells were then digested with 0.25% trypsin for 1~2 min, in which way, dental mesenchymal cells (DMCs) were digested and most of epithelial cells were still adherent to the plastic surface of the cell culture dish. The digested cells were further cultured in the above medium without any antibiotic/antimycotics. Due to the difference in the sensitivity to trypsin and medium requirement, the residual epithelial cells gradually lost from the culture, leaving only the mesenchymal cells.[40] DMCs of passage 3 were used for further experiments. For the following in vivo studies (nude mice), the cells of passage 3 were cultured with DMEM/F12 (1:1) medium supplemented with 10% FBS, 10ng/ml TGF-β1 and 10mM glycerol 2-phosphate disodium salt hydrate (β-GP) (Sigma).

Identification of cultured DMCs

DMCs of third passage were seeded onto coverslips and cultured to almost 80%~90% confluence, and then the cells were fixed in 4% paraformaldehyde for 10 min. The subsequent steps for cell staining were performed according to the manufacturer;s instructions. Briefly, the primary antibody against Vimentin, a marker for

mesenchymes,[41, 42] was monoclonal anti-Vimentin antibody produced in mouse (Sigma), and the second antibody used was Alexa Fluor® 488 Goat Anti-Mouse IgG(H+L) (Invitrogen). Propidium iodide (PI) was used for counterstaining. The sample was then examined using a confocal laser scanning microscope (Nikon, A1).

Preparation of injectable HAG scaffold

HA was first dissolved in 1% NaOH at a concentration of 10 wt%, after which BDDE was added to the HA solution with a final concentration of 0.4 vol%. The solution was then allowed to crosslink at 40°C for 5h followed by being dried at room temperature for 3 days. Phosphate buffered saline (PBS: NaCl, 9mg/ml; KH_2PO_4, 0.03mg/ml; $Na_2HPO_4 \times 2H_2O$, 0.14 mg/ml; pH=7) of 500 ml was then added to the cross-linked HA to make it swell, after which the crosslinked HA was put into dialysis bag and dialyzed sequentially with excessive deionized water and PBS sequentially to remove the residual BDDE. The resulting gel was adjusted with PBS to a concentration of 20 mg/ml and then smashed with a homogenizer to prepare gel particles of 0-400μm. The yielded HAG was then sealed and stored at 4°C for the standby application. Before being used in cell or animal experiments, HAG was sterilized in a high-pressure steam sterilizer set at 120°C, 20 min.

Regeneration of dentin-pulp complex subcutaneously in nude mice using injectable HAG scaffold

The above cultured third passage DMCs were mixed with HAG scaffold (pre-incubated at 37°C for 3h) at a ratio of 5×10^7 cells/ml scaffold, further supplemented with 1μg/ml TGF-β1. The resulting cell-scaffold composite was immediately injected subcutaneously into the dorsum of ~5 weeks old male nude mice (Experimental) for 7 or 10 weeks. At the same time, cell-scaffold complex without TGF-β1 (Control 1) or HAG scaffold only (Control 2) similarly injected into nude mice were used as controls. Each of the above three groups had 10 samples of 7 w and had 10 samples of 10 w.

Moreover, in the experimental group, the cell concentration was varied (2.5×10^7 cells/ml, 1×10^7 cells/ml and 5×10^6 cells/ml) to investigate its effect on subsequent neo-tissue regeneration. Each condition of these three concentrations had 4 repeated

samples.

Preparation of β-TCP scaffold to engineer dentin-pulp complex subcutaneously in nude mice

The sterile β-TCP (Bio-lu, Shanghai, China) was cut into around $5\times5\times5mm^3$ in size and then coated with pre-prepared 0.1% Collagen I (containing 1μg/ml TGF-β1) at 4^oC overnight, after which the coated scaffold was washed with DMEM/F12 (1:1) medium once and dried in clean bench before usage. The collagen solution for coating was prepared as follows: powder of Collagen I from rat tail (C7661, Sigma) was dissolved in 0.1M acetic acid and sterilized with chloroform at 4^oC overnight. The sterilized Collagen I in the supernate was then gently removed to a sterile centrifugal tube and adjusted to a concentration of 1mg/ml at pH 7.2. TGF-β1 was then added to this collagen solution at a concentration of 1μg/ml. The prepared Collagen I solution was then stored at 4^oC for subsequent coating.

The above cultured third passage DMCs were then seeded onto this coated β-TCP scaffold with a cell density of 5×10^7 cells/cm^3. The composite was then placed in a 6-well plate. One ml of the TGF-β1 supplemented DMEM/F12 (1:1) medium was added into the well after being incubated for 4 h to allow cell attachment. The β-TCP composite was then implanted subcutaneously into the dorsum of ~5 weeks old male nude mice for 7 or 10 weeks, respectively. At each time point, 4 samples were repeated.

Preparation of PGA scaffold to engineer dentin-pulp complex subcutaneously in nude mice

As described previously,[43] fifteen milligrams of non-woven PGA fibers (Shanghai Jurui Biomaterials Company Inc., Shanghai, China) were pressed into meshes of approximately 9 mm in diameter and 1 mm in height. To improve its stability, PLA at a concentration of 0.5% in chloroform was added to the PGA mesh by dropping at a ratio of 10% of the total weight. The solvent was allowed to evaporate, and the resulting scaffolds were sterilized using 75% ethanol for 1 h and rinsed 3 times with PBS. Before cell seeding, the scaffolds were immersed in DMEM/F12 (1:1) medium overnight before usage.[43]

DMCs of third passage were then seeded onto this stabilized PGA scaffold with a cell density of 5×10^7 cells/cm^3. The composite was then placed in a 6-well plate. One ml of the TGF-β1 supplemented DMEM/F12 (1:1) medium was added into the well after being incubated for 4 h to allow cell attachment. The PGA composite was then implanted subcutaneously into the dorsum of ~5 weeks old male nude mice for 7 or 10 weeks, respectively. At each time point, 4 samples were repeated.

Regeneration of dentin-pulp complex within pre-treated tooth slices

Preparation of tooth slices: Noncarious human second premolars were collected from the patients of the Oral Surgery Clinic in Shanghai Ninth People's Hospital Affiliated Shanghai Jiao Tong University School of Medicine. The residual gingiva and periodontal tissues were removed with a scalpel, and the teeth were then cut at the cervical region with a high-speed turbine to obtain slices of approximately 1mm in thickness. The pulp was thoroughly removed with dental barbed broaches from the above slices. The resulting tooth slices were soaked in 75% ethanol for 1 h and washed with sterile dulbecco's phosphate buffered saline (D-PBS) (NaCl: 8.0g/L, KCl: 0.2g/L, KH_2PO_4: 0.2g/L, Na_2HPO_4((anhydrous): 1.15g/L, pH=7.2)(Sigma-Aldrich) for several times. After that, the tooth slices were preincubated with DMEM/F12 (1:1) medium with 15% FBS at an incubator set at 37°C and 5% CO_2 for several hours before subsequent usage.

DMCs of third passage were mixed with HAG scaffold (pre-incubated at 37°C for 3h) at a ratio of 5×10^7 cells/ml scaffold, further supplemented with 1μg/ml TGF-β1. This cell-scaffold composite was first injected into the empty cavity of prepared tooth slice, and the resulting slice was then implanted subcutaneously into the nude mice for 10 weeks. As to this tooth slice model, five samples were repeated.

Regeneration of dentin-pulp complex in porcine dental pulp cavity

For the dentin-pulp regeneration in mini pigs, the unerupted permanent molar tooth buds of 3-month-old mini pigs were surgically removed from mandibles, and then digested and cultured according to the same way mentioned above. For the following in vivo studies, the obtained DMCs of third passage were cultured with DMEM/F12 (1:1) medium supplemented with 10% FBS, 10 ng/ml TGF-β1 and 10mM β-GP.

Treatment of porcine dental pulp cavity: The same 3-month old porcine after removal of unerupted permanent tooth buds was anesthetized with 0.25% pentobarbital sodium. Dental pulps of the second and third premolars in the mandible were removed with dental barbed broaches. The tooth canal space was enlarged and the cavity was temporarily sealed with hydraulic temporary restorative (GC, Japan) according to the routine clinical procedures.

At one week after the above dental pulp cavity treatment, the above third passage DMCs were mixed with HAG scaffold (pre-incubated at 37^{o}C for 3h) at a ratio of 5×10^{7} cells/ml scaffold, further supplemented with 1μg/ml TGF-β1. For the experimental group in this big animal study, this cell-scaffold composite was then injected into the empty porcine dental pulp cavity. Immediately before the injection, the temporarily sealing was removed and the pulp cavity was thoroughly washed with 5.25% NaClO, 3% H_2O_2 and sterile 0.9% NaCl in sequence. The prepared cell-scaffold composite was then injected into the pulp cavity and the hole was sealed with mineral trioxide aggregate (MTA) and glass ionomer cement (GC, Japan) sequentially. Moreover, clinical and blank controls were also conducted. The empty dental pulp cavity was similarly treated except filled with gutta percha points, which was served as a control of clinical treatments (Clinical control). The empty dental pulp cavity was also similarly treated except that the cavity was left empty as a blank control. All the pigs were normally raised after the above surgeries. After one month, the above implants were harvested for the following histological analysis. As to this mini pigs model, each of the three groups (EXP, Clinical and Blank) had 5 samples repeated.

Histology and immunohistochemical analysis

When it's time to harvest the samples, the animals were treated with euthanasia. The samples were then removed and washed with PBS, followed by being fixed in 4% paraformaldehyde at 4^{o}C for 24h, demineralized with 10% EDTA at room temperature for several months. The samples were then processed paraffin section, and the sections (5μm-thick) were performed H&E, Masson (MAIXIN.BIO) and immunohistochemical staining. The primary antibody used for the

immunohistochemical analysis is rabbit anti-human dentin sialoprotein (DSP) polyclonal antibody (H-300) (1:100 dilution) (Santa Cruz). The second antibody used was Envision+ system-HRP labeled polymer anti-rabbit (Dako), and liquid DAB+ substrate chromogen system (Dako) was used as well.

Quantitative real-time reverse transcriptase-polymerase chain reaction (RT-PCR)

To detect the expression of dentinogenesis related genes, *DSPP* (dentin sialophosphoprotein), *DMP-1* (dentin matrix protein 1), *MEPE* (matrix extracellular phosphoglycoprotein), and *BSP* (bone sialoprotein), samples of Experimental (DMC+HAG+TGF-β1) and Control 1 (DMC+HAG) groups which were subcutaneously constructed in nude mice for 10w were harvested. The respective total RNA was extracted using TRIzol® Reagent (Invitrogen, USA) from the samples, reverse-transcribed and amplified using a RevertAid First Strand cDNA Synthesis Kit (Thermo) in a 20-μL reaction mixture containing 1μl RNAase inhibitor, 1μl reverse transcriptase, 1μl oligo(dT)15, 2μl 10mM dNTPs, buffer and RNAase-free water. The PCR primers used here were purchased form Invitrogen Biotechnology Co., LTD. The detailed primer sequences were shown in Table 1. The expression of β-actin mRNA was used in all real-time PCR reactions as an internal control. The RT-PCR assay was performed using 7300 Real Time PCR System (Applied Biosystems) with the following profile: 95°C for 10min, and then cycling for 40 cycles at 95°C for 15 s and 60°C for 60s, and then 60°C for 5min. The relative expression of each mRNA was calculated by the ⊿Ct method. ⊿Ct is the value obtained by subtracting the Ct value of β–actin mRNA from the Ct value of the target mRNA.[44] The experiments were repeated three times and the values were the mean of 3 individual samples (n=3). Data are presented as mean ± SD.

Morphology of DMCs and injectable HAG scaffold

The cultured DMCs exhibited a typical spindle-shaped appearance as shown in Figure 1 A. Moreover, these cells were positive for vimentin, which is a characteristic protein of mesenchymal cells (Figure 1B). The sizes of prepared HAG particles were in the range of 0-400μm (Figure 1C), and these gels in the form of irregular microparticles could be easily injected via a syringe (30G) as shown in Figure 1 D.

Regeneration of dentin-pulp complex subcutaneously in nude mice

Gross views of samples of Experimental group which had been constructed subcutaneously in nude mice for 7 and 10 weeks were shown in Figure 2 A and D, respectively. Grossly, the engineered tissues of experimental group were highly mineralized both at 7 and 10 weeks. Therefore, before they were further subjected to histological staining, demineralization was necessary for obtaining paraffin slices. The implanted samples of Control 1 group (briefed as DMC+HAG) in nude mice for 7 and 10 weeks were shown in Figure 2 B and E. From the gross views (Figure 2 B and E), these samples were also mineralized and the mineralization degree was enhanced with time from 7w to 10w. The samples obtained from pristine HAG scaffold (Control 2, briefed as HAG) after 7 and 10 weeks; subcutaneous implantation in nude mice were shown in Figure 2 C and F. The harvested samples of this Control 2 group were soft and transparent. A high water content could be envisioned on samples for Control 2 group.

Overall view of H&E and Masson staining of the regenerated tissue of the Experimental group of 7 weeks were shown in Figure 3 A and D, respectively. The whole sample exhibited island-like features. Within localized areas of a higher magnification (Figure 3 B, C, E and F), there were well organized dentinal tubules (white arrow head), columnar odontoblast-like cells (yellow arrow head) with polarized basal nuclei and blood vessels (black arrow head). Those cells with polarized basal nuclei aligned against the regenerated dentin-like tissue, while those dentinal tubules (white arrow head) arranged radially from the pulp-like tissue.

No typical dentin or pulp like tissue can be seen in both Control 1 (Figure 4 A-C)

and Control 2 groups (Figure 4 D-F). For both groups, HAG (green arrow head) still occupied the most areas, but most of the HAG fragments would be missed during the H&E processing. A few bone-like hard tissue could be located within the DMC+HAG sample (Figure 4 B), whereas only fibrous soft tissue could be identified encapsulating the sample of HAG group (Figure 4 E and F).

When it came to 10 weeks, the regenerated tissue of the Experimental group exhibited a more mature feature of dentin-pulp like morphology as shown in Figure 5, compared to those of 7 weeks (Figure 3). From the overall view of H&E (Figure 5 A) and Masson (Figure 5 D) staining of the regenerated tissue, it can be seen that the formed typical island-like tissues were quite homogeneous throughout the whole sample. Moreover, as shown in Figure 5 B, C, E, and F (higher magnification observations of the localized square areas within A and D), in the regenerated construct there were well-organized dentinal tubules (white arrow head) arranged radially along the pulp-like tissue and columnar odontoblast-like cells with polarized basal nuclei (yellow arrow head) juxtaposed along the dentinal wall. Blood vessels could be observed with a well distribution within the pulp-like soft tissue (black arrow head).

As to the control groups of 10 weeks (Figure 6 A and D), similar conditions were observed as those of 7 weeks. A relatively high density of cells could still be observed in samples of Control 1 group (Figure 6 B and C), whereas only residues of HAG scaffolds could be located with fibrous encapsulation at the edge of the implants (Figure 6 E and F).

Based on the above results, immunohistochemical staining for DSP was carried out on the constructs of the experimental group which were implanted for 10 weeks. The results were then shown in Figure 7. Positive staining for DSP throughout the whole structure, especially within the area of soft tissue (Figure 7 A) could be ascertained. From the higher-magnification views (Figure 7 A1 and A2), the positive DSP expression by odontoblast-like cells (yellow arrow head) and dentinal tubules (white arrow head) could be confirmed. The negative immunohistochemical staining for Figure 7 A, A1, and A2 were shown in Figure 7 B, B1 and B2, respectively,

obtained by the similar processing except without the usage of antibodies, further confirming the specific staining. Moreover, positive control staining was carried out on slices obtained from a normal tooth of a 6-month pig as shown in Figure 7 C (Figure 7 D was respective negative staining for C), exhibiting positive staining for DSP in the pulp and dentinal tubules. The normal mature dentin-pulp structure and the regenerated tissue (experimental group in this study) bore great similarity in their microstructures and tissue distribution.

A few odonto-osteogenic and dentinogenesis related markers (*DSPP, DMP-1, MEPE, BSP)* were examined by RT-PCR and the results were shown in Figure 8. The expression of *DSPP, DMP-1, MEPE* and *BSP* in the experimental group (EXP) was highly elevated compared to those of the Control 1 group ($p<0.0001$ for each gene), confirming the odontoblastic differentiation of DMCs and dentinal formation within the regenerated tissue of EXP group.

The cell concentration was varied from original 5×10^7 cells/ml to 2.5×10^7 cells/ml, 1×10^7 cells/ml and 5×10^6 cells/ml, respectively, so as to investigate the effect of cell density within the HAG scaffold on the morphology of neo-formed tissue of the experimental group. Figure 9 then showed the gross view, histological and immunohistochemical analysis of regenerated tissue constructed subcutaneously in nude mice for 10 weeks with the minimum concentration used (5×10^6 cells/ml). Compared with those constructed from 5×10^7 cells/ml (Figure 2 D and Figure 5 A, D), only sporadically-distributed tissue was regenerated within the whole sample (Figure 9 A, B and D). In the higher magnification observations (Figure 9 C, E) of the localized square areas within Figure 9 B and D, dentinal tubules (white arrow head) and columnar odontoblast-like cells (yellow arrow head) could also be identified along the island-like structure, despite of their relatively lower density. Moreover, the presence of blood vessels could be ascertained (black arrow head) as well. According to the immunohistochemical analysis (Figure 9 F), positive DSP expression by the polarized odontoblast-like cells (yellow arrow head) and dentinal tubules (white arrow head) in the regenerated tissue could be observed. From the rest samples constructed from 2.5×10^7 cells/ml and 1×10^7 cells/ml, similar conditions were observed that the

microstructure of neo-tissues had similar features to that constructed from 5×10^7 cells/ml, but the quantity of expected tissue decreased with the reduction in cell density (data not shown).

To further verify the suitability of HAG as a scaffold for dentin-pulp regeneration, two commonly used scaffolds, β-TCP and PGA were applied as scaffold controls. The gross view, histological and immunohistochemical analysis of regenerated tissue constructed with DMC (5×10^7 cell/ml), TGF-β1 (1μg/ml) and β-TCP as a scaffold in mouse subcutaneously model were shown in Figure 10. Grossly, most of the constructs at either 7 or 10 weeks were still β-TCP scaffolds. The gross shape of constructs was still remained as that of the original scaffold (Figure 10 A and B). Microscopically, it was shown that no observable pulp or dentin-like tissue could be identified within this construct from H&E (Figure 10 A1) and Masson staining (Figure 10 A2) except that weak staining for DSP around the cells within the construct was shown from immunohistochemical staining (Figure 10 A3). Even with the increase in the in vivo time, the tissue still did not undergo obvious remodeling into dentin-pulp like morphology (Figure 10 B1, B2 and B3) as observed from HAG constructed samples (Figure 5 A-F).

The gross view, histological and immunohistochemical analysis of regenerated tissue constructed with DMC (5×10^7 cell/ml), TGF-β1 (1μg/ml) and PGA as a scaffold in mouse subcutaneously model were shown in Figure 11. Grossly, PGA fibers could still be observed within the construct at 7 weeks (Figure 11 A). When it came to 10 weeks, it seemed that most of PGA fibers were degraded, but the tissue was quite soft (Figure 11 B). Microscopically, similarly as those observed from Figure 10 using β-TCP as a scaffold, no typical pulp or dentin-like tissue could be observed within this construct except weak staining for DSP both at 7 (Figure 11 A1-A3) and 10 weeks (Figure 11 B1-B3). Interestingly, the tissue microstructure varied with time. At 7 weeks, compact and hard bony like tissue was formed and surrounded by fibrous soft tissue entrapped with a high density of cells (Figure 11 A1-A3), whereas at 10 weeks the previous hard tissue became relatively soft with a cartilage-like appearance in both tissue features and cell distribution.

Regeneration of dentin-pulp complex subcutaneously in tooth slice model

To further investigate the effect of microenvironment on tissue regeneration, the cell scaffold composite (DMC+HAG+TGF-β1) was injected into a pre-prepared tooth slice and then implanted into the subcutaneous area of a nude mouse as shown in Figure 12 A-C. After being implanted for 10 weeks, the tooth slice was harvested (Figure 12 D). Grossly, the empty pulp chamber of the tooth slice was filled with regenerated tissue, which was further confirmed by H&E (Figure 12 E) and Masson (Figure 12 F) staining. The regenerated tissue had dentinal tubules (white arrow head) arranged radially along the pulp chamber (Figure 13 A1 and B1). The neo-dentinal like tissue was in well integrity with the original dentin. Columnar odontoblast-like cells (yellow arrow head) with polarized basal nuclei aligned parallelly along the neo-dentinal like tissue with blood vessels distributed throughout the construct (black arrow head) (Figure 13 A1, A2, B1 and B2). Positive expression of DSP by polarized odontoblast-like cells (yellow arrow head) and dentinal tubules (white arrow head) could be observed (Figure 13 C1 and C2).

Regeneration of dentin-pulp complex in porcine dental pulp cavity

In order to investigate whether the current injectable scaffold had the clinical reference, the cell scaffold composite (DMC+HAG+TGF-β1) was finally injected into the empty tooth pulp chamber of a minipig. After one month, the tooth with the injected composite was retrieved as shown in Figure 14 A and A1. From the higher magnification H&E (A2, A3) and Masson (A4) observations of the regenerated tissue of this EXP group, multiple layers of columnar odontobalst-like cells (yellow arrow head) with polarized basal nuclei were well-aligned against the regenerated dentin-like tissue. Vivid regeneration of neo-dentin structure (white arrow) could be indicated and the neo-tissue was in well integration with the original dentin. The tubule morphology in the neo-dentinal structure could be observed obviously (white arrow head, Figure 14 A4). The distribution of blood vessels (black arrow head) in the pulp tissue can be observed (Figure 14 A2-A4). As a clinical control, gutta percha points were inserted into the similarly pre-prepared empty pulp chamber of minipig and also constructed for one month (Figure 14 B). However, the original dentin

remained destroyed or was still in the process of degradation according to the H&E (Figure 14 B1-B3) and Masson (Figure 14 B4) staining. No dentin and pulp like tissue was regenerated in this chamber. As to the blank control group (Figure 14 C), of which the empty pulp chamber after the removal of pulp tissue via routine clinical procedures was left untreated, no tissue regeneration was observed in the chamber from the overall histological morphology (Figure 14 C1), higher magnification H&E (Figure 14 C2 and C3) and Masson (Figure 14 C4) observations.

Polarized histological morphology of the regenerated dentin-pulp complex in the empty tooth pulp chamber of minipig was shown in Figure 15. Figure 15 A and D were two representative images, while B, C, E, and F were images of higher magnifications. From Figure 15 A and D, it could further confirm the vivid regeneration of neo-dentin structure. The neo-dentinal tissue was in well integration with the original dentin, but has distinctive polarized morphology. From the higher magnification (B, C, E, and F), the tubule morphology in the neo-dentinal structure had similar organization and distribution to that in the original dentine.

Discussion

In this report, an injectable tissue engineering method was developed for dentin-pulp complex structure regeneration via the application of an injectable scaffold, HAG. It was then demonstrated that dentin-pulp like tissue with typical well organized dentinal tubular structures, columnar odontoblast-like cells were successfully engineered within the subcutaneously area of nude mice using HAG, DMCs and TGF-β1. It was also found that with time from 7 to 10 w, the neo-tissue remodeled and further organized. Sufficient amount of DMCs is necessary for the formation of desired tissue as illustrated by experiments of reducing the cell density till 5×10^6 cells/ml scaffold. The efficacy of such injectable tissue engineering method was also demonstrated in empty tooth slices and pulp chambers of mini pigs which had been pre-treated by thoroughly removing pulp using dental barbed broaches. Not only vivid growth of neo-dentin and pulp like tissue was realized, but also well integrity with the original dentin was achieved. Hence, the suitability of an injectable scaffold, HAG, for dentin-pulp complex engineering was ascertained, and its superiority of easy penetrating and delivering DMCs and TGF-β1 into the whole pulp canal with minimum invasion over traditional β-TCP and PGA scaffolds with rigid shapes was substantiated. As is known, for decades, various efforts had been paid on dentin-pulp regeneration. However, the dream to engineer the whole pulp was hampered by the specific anatomical arrangement of pulp and dentin, which could then overcome by the current usage of an injectable scaffold, HAG.

In addition to the specific anatomical and clinical requirements that the injectable HAG scaffold meets, the suitability of HAG further lie in its appropriate degradation rate. Based on the histological observation of the experimental group in nude mice, it seems that most of the HAG fragments were already gone, whereas the majority was still remained in the control group (HAG only). One indication is that HAG properly degraded in a speed keeping pace with the rate of dentin-pulp complex regeneration. The other is that HAG could possibly have the flexibility to adjust its degradation under different environments. That is, cells or extracellular matrix within HAG

scaffold could easily help to adjust its turnover, probably due to the biological nature of HA. What's more, the degradation product of HAG is HA of different molecular weights. As one type of the glycosaminoglycans present in the extracellular matrix, HA was shown to be beneficial to maintain morphologic organizations by preserving extracellular spaces and was reported to contribute to the initial development of dentin matrix and dental pulp.[4, 23] Hence, most probably, the degradation products of HA might also facilitate the matrix formation process. As to the two commonly used scaffolds, β-TCP and PGA, no typical dentin or pulp-like tissue regeneration was observed subcutaneously in nude mice after 7 or 10 weeks. One possible reason of this might be due to their different chemical properties. As is known, when PGA degraded, the acid product might influent the metabolism of the cells in the construct and may thereby hamper the regeneration of dentin-pulp complex under the same circumstance. β-TCP has the osteoinductive property and was shown to be beneficial for bone regeneration,[6] but may not be appropriate for dentin-pulp regeneration as the pulp is a type of soft tissue. According to our results, even at 10 weeks subcutaneously, β-TCP still remained its original structure. Such a low degradation rate under such circumstances could be one of the main reasons that hampered the neo-tissue regeneration and reorganization.

DMCs were derived from ectomesenchyme during tooth development, and these cells hold the ability to differentiate into dentin-secreting odontoblasts.[2, 45-47] They could also form dental pulp like tissue with good vascularization, which is important in regulation of inflammation, subsequent regeneration of pulp and dentin, and in sustaining the high metabolic demands of odontoblastic cells during active processes of dentin matrix secretion.[48, 49] Therefore, tooth bud cells have been widely used for tooth development and regeneration research.[7, 50-53] In this study, DMCs from the newly born porcine or from unerupted permanent tooth buds of 3-month old mini pigs were used as seed cells for dentin-pulp regeneration in subcutaneous area of nude mice or empty pulp chamber of pigs, respectively. However, no detailed characterizations of these cells were carried out to identify their differentiation status along with the neo-tissue formation, thereby monitoring their fate and exact roles.

This will be one of our following issues to be explored. In order to bridge the gap between research and clinical applications, alternative seed cells should also be developed, such as postnatal dental pulp stem cells (DPSCs), stem cells from human exfoliated deciduous teeth (SHED), stem cells from apical papilla (SCAP), bone marrow derived mesenchymal stem cells (BMSCs) and adipose derived stem cells (ASCs).[2, 54-58]

It was shown that TGF-β family plays important roles in tooth development. Among which, TGF-β1 was shown to promote odontoblast differentiation and the subsequent secretion of extracellular matrix components. It also enhances the formation of reparative dentin and is essential for the homeostasis of the dentin-pulp complex.[37, 38, 59, 60] Moreover, as reported, TGF-β1 was crucial in the terminal odontoblast differentiation of pulp cells in vitro.[61] Due to its important role in tooth morphogenesis, TGF-β1 was taken as a morphogen in this report to promote dentin-pulp complex regeneration. As confirmed by current results, well vascularized dentin-pulp complex regeneration in nude mice model of the experimental group (DMCs+HAG+TGF-β1) was achieved, whereas no dentin or pulp but only bone-like tissue formation was observed in the control group (DMC+HAG) without any TGF-β1.

The gene expression levels of *DSPP, DMP-1, MEPE* and *BSP,* indicative of odontoblast differention and dentin-pulp regeneration,[5, 6, 33, 62] of the subcutaneously regenerated dentin-pulp like tissue were assessed. *DSPP* is one of the key non-collagenous proteins involved in tooth development and is critical for dentin mineralization.[63-65] *DMP-1*, involved in the initial phase of mineralized dentin formation, was shown to induce the undifferentiated pulp cells into matrix-synthesizing cells and to stimulate the formation of mineralized tissues.[66, 67] *MEPE*, an extracellular matrix protein that is mainly expressed in mineralized tissues and dental pulp, plays important roles not only in dentinogenesis but also in the physiology of the pulp homeostasis.[68, 69] *BSP* was reported to stimulate the differentiation of dental pulp cells into odontoblast-like cells and to stimulate regenerative dentin formation.[70-72] Quantitatively, their expression was remarkably

enhanced in the experimental group. This further helps to confirm the nature of regenerated dentinal and pulp like tissue, in addition to the observed characteristic tubular dentin morphology which is usually served as a hallmark of odontoblasts[73] as well as the positive immunostaining for DSP.

In this work, three different microenvironments were tried to assess the ability of HAG scaffolds to form dentin-pulp structure and to assess the preliminary clinical suitability. Firstly, subcutaneous area is usually used to make initial examination on cell- and tissue-based products in vivo because it offers simple transplantation surgeries compared with others and is easier to access.[74]The nude mouse subcutaneous model has also been widely used for partial tooth tissue regeneration, such as dentin, pulp and dentin-pulp complex regeneration.[75-77] Hence, in this report, it was firstly tried to substantiate our hypothesis that HAG could be used as an injectable scaffold to engineer dentin-pulp complex. To further make the microenvironment more close to the original one of dentin-pulp, pre-treated tooth slices were further applied. The tooth slice model has been used for several studies, such as for cytotoxicity assessment of dental materials,[78] for the study of dentinogenesis and human dental pulp angiogenesis.[79, 80] It is a suitable experimental model for mechanistic and translational studies which are focused on the use of stem cells for the understanding of dental pulp biology and dental pulp tissue engineering.[81] It is also a well-known model to address the clinical potential of stem cell transplantation, which has provided major insights into the use of scaffolds and stem cells in regenerative endodontics.[8, 82] Interestingly, growth of the dentin along the original one was demonstrated with neo-pulp like tissues being encased within the regenerated dentin in the current investigation. However, there were few scattered cells entrapped in the regenerated dentin. This phenomenon was reported by previous studies that in the de novo regenerated dentin odontoblast-like cells were sometimes entrapped in the reparative dentin during reparative dentin formation.[6, 83] Therefore, the newly regenerated dentin-like tissue in this tooth slice model may be similar to tertiary dentin. This second stage evaluation further strengthened our proposal and finally an in situ regeneration experimental model, empty pulp chamber after

thorough removal of pulp and part of dentin, was applied to verify its clinical applicability. Through the successful delivery of DMCs and TGF-β1 by injectable HAG scaffold, the porcine destroyed dentin was vividly repaired along with the formation of pulp-like tissues. It can then be concluded that the current injectable engineering method based on injectable HAG scaffolds would make great contribution to the future clinical regeneration of dentin-pulp complex in regenerative endodontics.

Acknowledgement of financial support:

This study is financially supported by National "973" Project Foundation (Grant No: 2010CB944804), "the Fundamental Research Funds for the Central Universities", and Foundations from Shanghai Science and Technology Development Committee (11QB1402200; 12411950700).

References

1. F. F. Demarco, M. C. Conde, B. N. Cavalcanti, L. Casagrande, V. T. Sakai and J. E. Nör, *Braz Dent J*, 2011, 22, 3-13.

2. G. T. Huang, *Front Biosci (Elite Ed)*, 2011, 3, 788-800.

3. H. H. Sun, T. Jin, Q. Yu and F. M. Chen, *J Tissue Eng Regen Med,* 2011, 5, e1-16.

4. C. Kitamura, T. Nishihara, M. Terashita, Y. Tabata and A. Washio, *Int J Dent,* 2012, 190561.

5. V. Rosa, Z. Zhang, R. H. Grande and J. E. Nör, *J Dent Res*, 2013, 92, 970-5.

6. G. T. Huang, T. Yamaza, L. D Shea, F. Djouad, N. Z. Kuhn, R. S. Tuan and S. Shi, *Tissue Eng Part A*, 2010, 16, 605-15.

7. T. F. Kuo, A. T. Huang, H. H. Chang, F. H. Lin, S. T. Chen, R.S. Chen, C. H. Chou, H. C. Lin, H. Chiang and M. H Chen, *J Biomed Mater Res A*, 2008, 86, 1062-8.

8. M. M. Cordeiro, Z. Dong, T. Kaneko, Z Zhang, M. Miyazawa, S. Shi, A. J Smith and J. E. Nör, *J Endod*, 2008, 34, 962-9.

9. Y. Zheng, X. Y. Wang, Y. M. Wang, X. Y. Liu, C. M. Zhang, B. X. Hou and S. L. Wang, *J Dent Res*, 2012, 91, 676-82.

10. J. Ghoddusi, M. Forghani and I. Parisay, *Iran Endod J,* 2014, 9, 15-22.

11. G. T. Huang, *Regen Med*, 2009, 4, 697-707.

12. W. Liu and Y. Cao, *Biomaterials*, 2007, 28, 5078-86.

13. C. M. Murphy, F. J. O'Brien and D. G. Little, *Eur Cell Mater*, 2013, 26, 120-32.

14. Ma. Peter X, *Materials Today*, 2004, 7, 30-40.

15. F. Baino and C. Vitale-Brovarone, *Acta Biomater*, 2014, 10, 3372-97.

16. C. Liu, Z. Xia and J. T. Czernuszka, *Chemical Engineering Research and Design*, 2007, 85, 1051-1064.

17. T. Garg, O. Singh, S. Arora and R. Murthy, *Crit Rev Ther Drug Carrier Syst*, 2012, 29, 1-63.

18. J. S. Colombo, A. N. Moore, J. D. Hartgerink and R. N. D'Souza, *J Endod*, 2014,

40(4 Suppl), S6-12.

19. E. Piva, A. F. Silva and J. E. Nör, *J Endod*, 2014, 40(4 Suppl), S33-40.

20. S. R. Simon, A. Berdal, P. R. Cooper, P. J. Lumley, P. L. Tomson and A. J. Smith, *Adv Dent Res*, 2011, 23(3), 340-5.

21. K. M. Galler, A. Eidt and G. Schmalz, *J Endod*, 2014, 40(4 Suppl), S41-5.

22. G. Schmalz and A. J. Smith, *J Endod*, 2014, 40(4 Suppl), S2-5.

23. N. Sakamoto, H. Okamoto and K. Okuda, *J Dent Res*, 1979, 58, 646-55.

24. S. Felszeghy, M. Hyttinen, R. Tammi, M. Tammi and L. Módis, *Eur J Oral Sci*, 2000, 108, 320-6.

25. J. A. Burdick and G. D. Prestwich, *Adv Mater*, 2011, 23, H41-56.

26. A. La Gatta, C. Schiraldi, A. D. Papa, A. Agostino, M. Cammarota, A. De Rosa and M. De Rosa, *Carbohydr Polym*, 2013, 96, 536-44.

27. X. Xu, A. K. Jha, D. A. Harrington, M. C. Farach-Carson and X. Jia, *Soft Matter*, 2012, 8, 3280-3294.

28. K. De Boulle, R. Glogau, T. Kono, M. Nathan, A. Tezel, J. X. Roca-Martinez, S. Paliwal and D. Stroumpoulis, *J Dent Res*, 1979, 58, 646-55.

29. K. Otsu, R. Kishigami, A. Oikawa-Sasaki, S. Fukumoto, A. Yamada, N. Fujiwara, K. Ishizeki and H. Harada, *Stem Cells Dev*, 2012, 21, 1156-64.

30. H. Yamazaki, M. Tsuneto, M. Yoshino, K. Yamamura and S. Hayashi, *Stem Cells*, 2007, 25(1), 78-87.

31. H. Imai, N. Osumi-Yamashita, Y. Ninomiya and K. Eto, *Dev Biol*, 1996, 176, 151-65.

32. M. T. Duailibi, S. E. Duailibi, C. S. Young, J. D. Bartlett, J. P. Vacanti and P. C. Yelick, *J Dent Res*, 2004, 83, 523-8.

33. C. S. Young, S. Terada, J. P. Vacanti, M. Honda, J. D. Bartlett and P. C. Yelick, *J Dent Res*, 2002, 81, 695-700.

34. M. J. Honda, H. Fong, S. Iwatsuki, Y. Sumita and M. Sarikaya, *Med Mol Morphol*, 2008, 41, 183-92.

35. M. J. Honda, T. Ohara, Y. Sumita, T. Ogaeri, H. Kagami and M. Ueda, *J Oral*

Maxillofac Surg, 2006, 64, 283-9.

36. I. Miletich and P. T. Sharpe, *Birth Defects Res C Embryo Today*, 2004, 72, 200-12.

37. W. He, J. Zhang, Z. Niu, Q. Yu, Z. Wang, R. Zhang, L. Su, L. Fu, A. J. Smith and P. R. Cooper, *J Dent Res*, 2014, 93, 496-501.

38. A. J. Sloan and A. J. Smith, *Arch Oral Biol*, 1999, 44, 149-56.

39. B. R. Snyder, P. H. Cheng, J. Yang, S. H. Yang, A. H. Huang and A. W. Chan, *BMC Cell Biol*, 2011, 12, 39.

40. S. S. Prime and B. H. Toh, *J Cell Sci,* 1978, 33, 329-40.

41. M. J. Honda, Y. Sumita, H. Kagami and M. Ueda, *Arch Histol Cytol*, 2005, 68, 89-101.

42. L. Guo, J. Li, X. Qiao, M. Yu, W. Tang, H. Wang, W. Guo and W. Tian, *PLoS One*, 2013, 8, e62332.

43. G. Zhao, S. Yin, G. Liu, L. Cen, J. Sun, H. Zhou, W. Liu, L. Cui and Y. Cao, *Biomaterials*, 2009, 30, 3241-50.

44. Y. Bai, Y. Bai, K. Matsuzaka, S. Hashimoto, E. Kokubu, X. Wang and T. Inoue, *Cell Tissue Res*, 2010, 342, 221-31.

45. J. Jernvall and I. Thesleff, *Mech Dev*, 2000, 92, 19-29.

46. H. Peters and R. Balling, *Trends Genet*, 1999, 15, 59-65.

47. H. Yamamoto, E. J. Kim, S. W. Cho and H. S. Jung, *J Electron Microsc (Tokyo)*, 2003, 52, 559-66.

48. V. Rosa, T. M. Botero and J. E. Nör, *Int Dent J*, 2011, 61 Suppl 1, 23-8.

49 K. Iohara, M. Murakami, N. Takeuchi, Y. Osako, M. Ito, R. Ishizaka, S. Utunomiya, H. Nakamura, K. Matsushita and M. Nakashima, *Stem Cells Transl Med*, 2013, 2, 521-33.

50. K. Nakao, R. Morita, Y. Saji, K. Ishida, Y. Tomita, M. Ogawa, M. Saitoh, Y. Tomooka and T. Tsuji, *Nat Methods*, 2007, 4, 227-30.

51. E. Ikeda, R. Morita, K. Nakao, K. Ishida, T. Nakamura, T. Takano-Yamamoto, M. Ogawa, M. Mizuno, S. Kasugai, T. Tsuji, *Proc Natl Acad Sci U S A*, 2009, 106, 13475-80.

52. M. Oshima, M. Mizuno, A. Imamura, M. Ogawa, M. Yasukawa, H. Yamazaki, R. Morita, E. Ikeda, K. Nakao, T. Takano-Yamamoto, S. Kasugai, M. Saito, T. Tsuji, *PLoS One*, 2011, 6, e21531.

53. H. Yamamoto, E. J. Kim, S. W. Cho and H. S. Jung, *J Electron Microsc (Tokyo)*, 2003, 52, 559-66.

54. L. Peng, L. Ye and X. D Zhou, *Int J Oral Sci*, 2009, 1(1), 6-12.

55. W. Jing, L. Wu, Y. Lin, L. Liu, W. Tang and W. Tian, *Med Hypotheses*, 2008, 70, 540-2.

56. Z. Y. Li, L. Chen, L. Liu, Y. F. Lin, S. W. Li and W. D. Tian, *J Oral Maxillofac Surg,* 2007, 65, 494-500.

57. C. N. Hung, K. Mar, H. C. Chang, Y. L. Chiang, H. Y. Hu, C. C. Lai, R. M. Chu and M C. Ma, *Biomaterials*, 2011, 32, 6995-7005.

58. L.Wu, F. Zhu, Y. Wu, Y. Lin, X. Nie, W. Jing, J. Qiao, L. Liu, W. Tang, X. Zheng and W. Tian, *Cells Tissues Organs*, 2008, 187, 103-12.

59. Y. C. Hwang, I. N. Hwang, W. M. Oh, J. C. Park, D. S. Lee and H. H. Son, *J Mol Histol*, 2008, 39, 153-60.

60. A. Piattelli, C. Rubini, M. Fioroni, D. Tripodi and R. Strocchi, *Int Endod J*, 2004, 37,114-9.

61. H. Magloire, A. Joffre and F. Bleicher, *J Dent Res*, 1996, 75, 1971-8.

62. M. Goldberg and A. J. Smith, *Crit Rev Oral Biol Med*, 2004, 15, 13-27.

63. S. Suzuki, T. Sreenath, N. Haruyama, C. Honeycutt, A. Terse, A. Cho, T. Kohler, R. Müller, M. Goldberg and A. B. Kulkarni, *Matrix Biol*, 2009, 28, 221-9.

64. S. Y. Lee, S. Y. Kim, S. H. Park, J. J. Kim, J. H. Jang and E. C. Kim, *J Dent Res*, 2012, 91, 407-12.

65. M. Prasad, W. T. Butler and C. Qin, *Connect Tissue Res*, 2010, 51, 404-17.

66. D. Martini, A. Trirè, L. Breschi, A. Mazzoni, G. Teti, M. Falconi and A. Jr. Ruggeri, *Eur J Histochem*, 2013, 57, e32.

67. R. S. Prescott, R. Alsanea; M. I. Fayad, B. R. Johnson, C. S. Wenckus, J. Hao, A. S. John and A. George, *J Endod*, 2008, 34, 421-6.

68. H. Wang, N. Kawashima, T. Iwata, J. Xu, S. Takahashi, T. Sugiyama and H. Suda,

Biochem Biophys Res Commun, 2010, 398, 406-12.

69. H. Liu, W. Li, S. Shi, S. Habelitz, C. Gao and P. Denbesten, *Arch Oral Biol*, 2005, 50, 923-8.

70. E. Piva, A. F. Silva and J. E. Nör, *J Endod*, 2014, 40, S33-40.

71. F. Decup, N. Six, B. Palmier, D. Buch, J. J. Lasfargues, E. Salih and M. Goldberg, *Clin Oral Investig*, 2000, 4, 110-9.

72. A. J. Smith and H. Lesot, *Crit Rev Oral Biol Med*, 2001, 12, 425-37.

73. G. Schmalz and A. J. Smith, *J Endod*, 2014, 40, S2-5.

74. H. Obokata, M. Yamato, S. Tsuneda and T. Okano, *Nat Protoc*, 2011, 6, 1053-9.

75. M. Miura, S. Gronthos, M. Zhao, B. Lu, L. W. Fisher, P. G. Robey and S. Shi, *Proc Natl Acad Sci U S A*, 2003, 100, 5807-12.

76. K. M. Galler, A. Eidt and G. Schmalz, *J Endod*, 2014, 40, S41-5.

77. R. S. Prescott, R. Alsanea, M. I. Fayad, B. R. Johnson, C. S. Wenckus, J. Hao, A. S. John and George, *J Endod*, 2008, 34, 421-6.

78. P. E. Murray, P. J. Lumley, H. F. Ross and A. J. Smith, *Biomaterials*, 2000, 21, 1711-21.

79. A. J. Sloan, R. M. Shelton, A. C. Hann, B. J. Moxham and A. J. Smith, *Arch Oral Biol*, 1998, 43, 421-30.

80. S. B. Gonçalves, Z. Don, C. M. Bramant, G.. R. Holland, A. J. Smith and J. E. Nör, *J Endod,* 2007, 33, 811-4.

81. V. T. Sakai, M. M. Cordeiro, Z. Dong, Z. Zhang, B. D. Zeitlin and J. E. Nör, *Adv Dent Res,* 2011, 23, 325-32.

82. M. T. Albuquerque, M. C. Valera, M. Nakashima, J. E. Nör and M. C. Bottino, *J Dent Res*, 2014, 93, 1222-31.

83. S. Batouli, M. Miura, J. Brahim, T. W. Tsutsui, L. W. Fisher, S. Gronthos, P. G. Robey and S. Shi, *J Dent Res*, 2003, 82, 976-81.

Legend:

Figure 1. Microscopic observation of DMCs and injectable HAG scaffold. Optical microsopic observation of DMCs (A) and immunofluoresent staining of DMCs for vimentin (B). Optical microsopic observation of HAG microparticles (C) which could be injected (D) via a syringe (30G). Scale bars: 500μm in A and C, 200μm in B.

Figure 2. Gross views of regenerated constructs using HAG as scaffolds. Gross view of regenerated tissue constructed subcutaneously with DMC (5×10^7 cells/ml), HAG and TGF-β1 (1μg/ml) (Experimental group, briefed as EXP) in nude mice for 7 (A) or 10 weeks (D), respectively. Gross view of the subcutaneously implanted constructs using DMC (5×10^7 cells/ml) and HAG (Control group 1, briefed as DMC+HAG) in nude mice for 7 (B) or 10 weeks (E). Gross view of the pristine HAG scaffold (Control group 2, briefed as HAG) subcutaneously implanted in nude mice for 7 (C) or 10 weeks (F).

Figure 3. Histological analysis of the regenerated dentin-pulp complex like tissue (EXP) constructed subcutaneously in nude mice for 7 weeks. Overall view of H&E (A) and Masson (D) staining of the regenerated tissue of EXP group. Island-like features can be located in A and D. B, C, E, and F are higher magnification observations of the localized square areas within A and D, respectively. It was shown in B, C, E, and F that in the regenerated construct there were well-organized dentinal tubules (white arrow head), columnar odontoblast-like cells (yellow arrow head) with polarized basal nuclei and blood vessels (black arrow head). Scale bars: 1000 μm for A, D; 50 μm for B, C, E, F.

Figure 4. Histological analysis of the DMC+HAG (A-C) and HAG (D-F) subcutaneously implanted in nude mice for 7 weeks. No typical dentin or pulp like tissue can be seen in both control groups. For both groups, HAG (green arrow head) still occupied the most areas and most of the HAG fragments missed during the H&E processing. A few bone-like hard tissue could be located within the DMC+HAG sample, whereas only fibrous soft tissue could be identified surrounding the sample of HAG group. Scale bars: 1000 μm in A, D; 50 μm in B, C, D, E.

Figure 5. Histological analysis of the regenerated dentin-pulp complex like tissue (EXP) constructed subcutaneously in nude mice for 10 weeks. Overall view of H&E (A) and Masson (D) staining of the regenerated tissue of EXP group. The tissues had typical island-like features in A and D. B, C, E, and F are higher magnification observations of the localized square areas within A and D. It was shown in B, C, E, and F that in the regenerated construct there were well-organized dentinal tubules (white arrow head) arranged radially along the pulp-like tissue and columnar odontoblast-like cells with polarized basal nuclei (yellow arrow head) lining up along the dentinal wall. Blood vessels were distributed throughout the pulp-like soft tissue (black arrow head). Scale bars: 1000 μm for A, D; 50 μm for B, C, E, F.

Figure 6. Histological analysis of the DMC+HAG (A-C) and HAG (D-F) subcutaneously implanted in nude mice for 10 weeks. No typical dentin or pulp like tissue can be seen in both control groups. Quite a few bone-like hard tissue could be located within the DMC+HAG sample, whereas only fibrous soft tissue could be identified surrounding the sample of HAG group. HAG fragments (green arrow head) still occupied the most areas of the HAG group. Scale bars: 1000 μm in A, D; 50 μm in B, C, D, E.

Figure 7. Immunohistochemical analysis of the regenerated dentin-pulp complex like tissue constructed subcutaneously in nude mice for 10 weeks. (A) Over view of the immunohistochemical staining for dentin sialoprotein (DSP) in the tissue, and DSP positive staining could be observed throughout the whole structure, especially within the area of soft tissue. (A1, A2) are higher magnification observations of the localized square areas within (A) and (A1), respectively, further confirming the positive DSP expression by odontoblast-like cells (yellow arrow head) and dentinal tubules (white arrow head). (B, B1 and B2) are negative controls of A, A1, and A2 respectively, obtained by the similar processing except without the usage of antibody. (C) is a slice from normal tooth of a 6-month pig, exhibiting positive staining of DSP in the pulp and dentinal tubules as a positive immunostaining control. (D) is negative staining for C. Scale bars: 1000 μm for A and B; 100 μm for A1 and B1; 50 μm for A2, B2, C, and D.

Figure 8. Relative mRNA expression of *DSPP, DMP-1, MEPE* and *BSP* by RT-PCR in Experimental (DMC+HAG+TGF-β1) and Control 1 (DMC+HAG) groups. EXP represents the experimental group which was constructed subcutaneously with DMC (5×10^7 cells/ml), HAG and TGF-β1 (1μg/ml) in nude mice for 10 weeks. CTR represents the Control 1 group which was constructed subcutaneously with DMC (5×10^7 cells/ml) and HAG in nude mice for 10 weeks. The experiments were repeated three times and the values were the mean of 3 individual samples (n=3). Data are presented as mean ± SD.

Figure 9. Gross view, histological and immunohistochemical analysis of regenerated tissue constructed subcutaneously with DMC (5×10^6 cells/ml), HAG and TGF-β1 (1μg/ml) in nude mice for 10 weeks. (A) Gross view of the constructed sample; Overall view of H&E (B) and Masson (D) staining of the sample, showing the sporadic tissue regeneration morphology within the whole construct. (C, E) are higher magnification observations of the localized square areas within B and D. A high cell concentration, dentinal tubules (white arrow head) and columnar odontoblast-like cells (yellow arrow head) could also be identified along the island-like structures. Moreover, the presence of blood vessels could be ascertained (black arrow head) as well. According to the immunohistochemical analysis (F), positive but relatively weak DSP expression by the polarized odontoblast-like cells (yellow arrow head) and dentinal tubules (white arrow head) in the regenerated tissue could be observed. Scale bars: 1000 μm in B and D; 50 μm for C, E, and F.

Figure 10. Gross view, histological and immunohistochemical analysis of regenerated tissue constructed with DMC (5×10^7 cells/ml), TGF-β1 (1μg/ml) and β-TCP as a scaffold in mouse subcutaneously model. Gross view of the regenerated tissue after being implanted in nude mice for 7 (A) and 10 (B) weeks, respectively. Insets in A and B were respective overall H&E staining of A and B. H&E staining of the formed tissue using β-TCP as a scaffold after being constructed for 7 (A1) and 10 (B1) weeks. Masson staining of the formed tissue after being constructed for 7 (A2) and 10 (B2) weeks. Immunohistochemical staining for DSP of the formed tissue after being constructed for 7 (A3) and 10 (B3) weeks. No observable pulp or dentin-like tissue could be identified within this construct, and weak staining for DSP around the cells within the construct was shown. Scale bars: 50μm for A1-A3 and B1-B3.

Figure 11. Gross view, histological and immunohistochemical analysis of regenerated tissue constructed with DMC (5×10^7 cells/ml), TGF-β1 (1μg/ml) and PGA as a scaffold in mouse subcutaneously model. Gross view of the regenerated tissue after being implanted in nude mice for 7 (A) and 10 (B) weeks, respectively. Insets in A and B were respective overall H&E staining of A and B. H&E staining of the formed tissue using PGA as a scaffold after being constructed for 7 (A1) and 10 (B1) weeks. Masson staining of the formed tissue after being constructed for 7 (A2) and 10 (B2) weeks. Immunohistochemical staining for DSP of the formed tissue after being constructed for 7 (A3) and 10 (B3) weeks. No typical pulp or dentin-like tissue could be observed within this construct except weak staining for DSP. Scale bars: 50μm for A1-A3 and B1-B3.

Figure 12. Process chart of dentin-pulp complex like tissue regeneration in tooth slice model. (A) The prepared tooth slice with an empty pulp chamber. (B) The pulp chamber of the prepared tooth slice was filled with the cell-scaffold composite (5×10^7 cells/ml DMC, HAG and 1μg/ml TGF-β1). (C) Implantation of the tooth slice subcutaneously into nude mice. (D) The harvested tooth slice after being implanted for 10 weeks. Overall views of H&E (E) and Masson (F) staining of the harvested tooth slice. Scale bars: 1000μm.

Figure 13. Histological and immunohistochemical analysis of the tissue regenerated in the pulp chamber of tooth slice model. H&E (A1, A2) and Masson (B1, B2) staining of the regenerated tissue in the pulp chamber of the empty tooth slice. The original empty chamber was filled with regenerated dentin pulp like tissue where dentinal tubules (white arrow head) arranged radially along the pulp chamber. The neo-dentinal like tissue was in well integrity with the original dentin. Columnar odontoblast-like cells (yellow arrow head) with polarized basal nuclei aligned parallelly along the neo-dentinal like tissue with blood vessels distributed throughout the construct (black arrow head). (C1, C2) Immunohistochemical staining for DSP of the regenerated dentin-pulp like tissue. Positive expression of DSP by polarized odontoblast-like cells (yellow arrow head) and regenerated dentinal tubules (white arrow head) could be observed. There were also HAG fragments remained within the pulp tissue (green arrow head). Scale bars: 50μm.

Figure 14. Regeneration of dentin-pulp complex in the empty tooth pulp chamber of minipig. Gross view (A) and overall histological morphology (A1) of the tooth implanted with 5×10^7 cells/ml of autologous DMC, HAG and 1μg/ml of TGF-β1 (EXP) by injection into the tooth pulp chamber of minipig for one month. Higher magnification H&E (A2, A3) and Masson (A4) observations of the regenerated tissue of the EXP group. Multiple layers of columnar odontobalst-like cells (yellow arrow head) with polarized basal nuclei were well-aligned against the regenerated dentin-like tissue. Vivid regeneration of neo-dentin structure could be thus indicated and the neo-tissue was in well integration with the original dentin (white arrow). The distribution of blood vessels (black arrow head) in the pulp tissue can be observed. Gross view (B) and overall H&E morphology (B1) of the tooth implanted with gutta percha points (as a clinical control) in the tooth pulp chamber of minipig for one month. Higher magnification histological (B2, B3) and Masson (B4) observations of the tooth of the clinical control group. No dentin or pulp like tissue was regenerated in this chamber, and the original dentin remained destroyed or was still in the process of degradation. Gross view (C) and overall H&E morphology (C1) of the tooth with its empty pulp chamber remained untreated (Blank control). Higher magnification H&E (C2, C3) and Masson (C4) observations of the tooth of the blank control group. Similar as those of the clinical control group, nothing was regenerated in the pulp chamber. Scale bars: 1000 μm in A1, B1, C1; 50μm in A2-A4, B2-B4, C2-C4.

Figure 15. Polarized histological morphology of the regenerated dentin-pulp complex in the empty tooth pulp chamber of minipig. The regenerated tissue was of the tooth implanted with 5×10^7 cells/ml of autologous DMC, HAG and 1μg/ml of TGF-β1 (EXP) by injection into the empty tooth pulp chamber of minipig for one month. B, C, E, and F are higher magnification polarized H&E observations of A and D, respectively. Scale bars: 200 μm for A and D; 100 μm for B and E; 50μm for C and F.

Table 1. Primer Sequences Used in Quantitative Real-time RT-PCR

Gene	Primers	Length
DSPP (NM_213777.1)	Forward: 5'-ATAGAGGACACCCAGAAACCCA-3' Reverse: 5'-GTCCAGGCTTATTTCCGGGT-3 '	295
DMP-1 (NM_001129953.1)	Forward: 5'-TGAGCAGGACAGCCCATCTG-3' Reverse: 5'-AGTAGCCGTCCTGGCAGTCATT-3'	212
MEPE (XM_003129339)	Forward: 5'-ACAGAGTTTTCCAGCCCAAGT-3' Reverse: 5'-CCCTGGTTCCAATGGTATCTC-3'	115
BSP (XM_003129337.1)	Forward: 5'-ACAAGCACGCCTACTTCTACCC-3' Reverse: 5'-TGGAGGGCAGCGAGACCTAT-3'	274
ACTB (XM_003124280)	Forward: 5'-TTCGAGACCTTCAACACCC-3' Reverse: 5'-CATGAGGTAGTCGGTCAGGT-3'	201

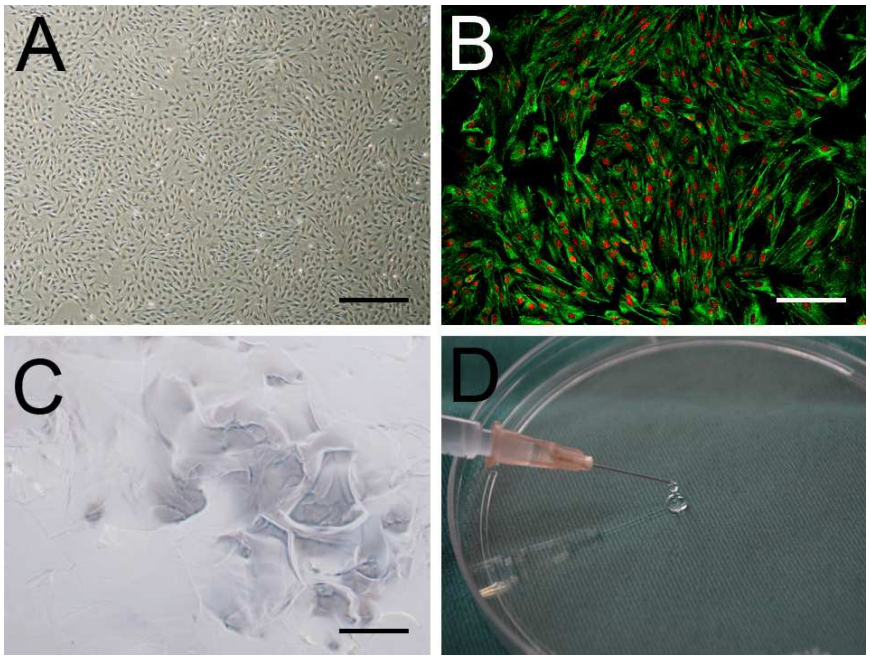

Figure 1

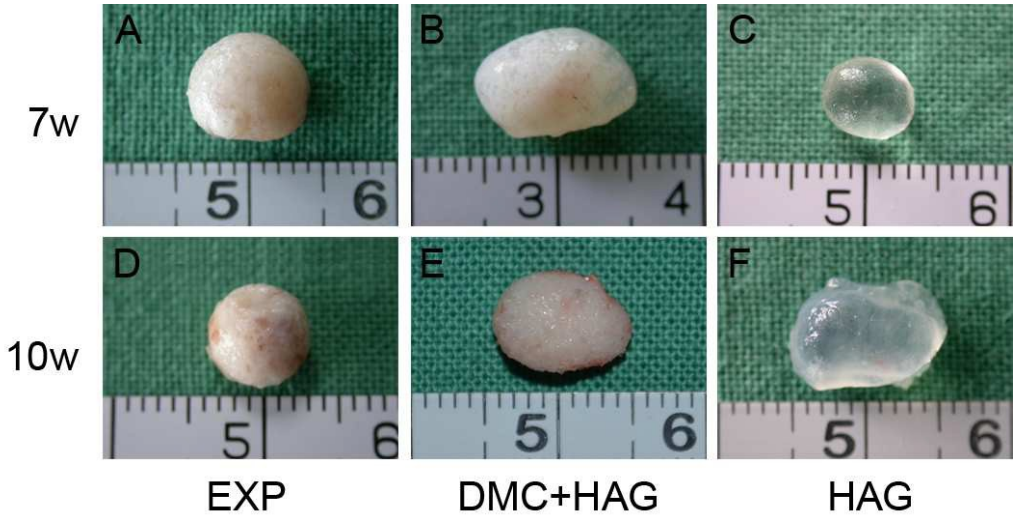

Figure 2

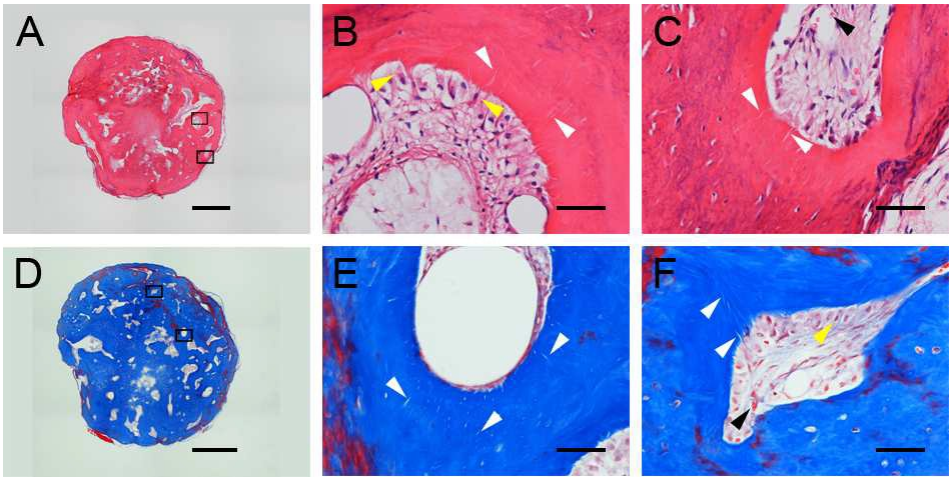

Figure 3

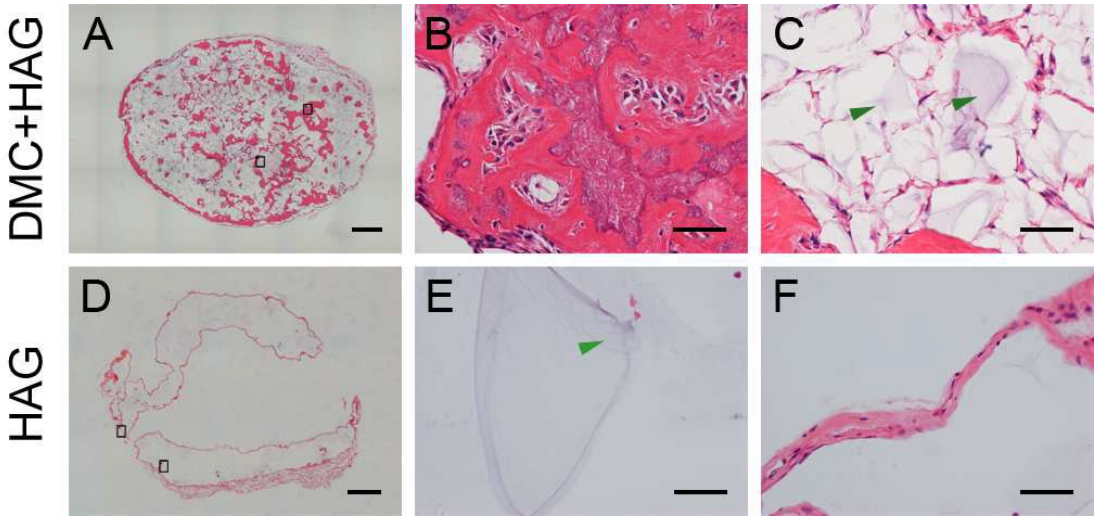

Figure 4

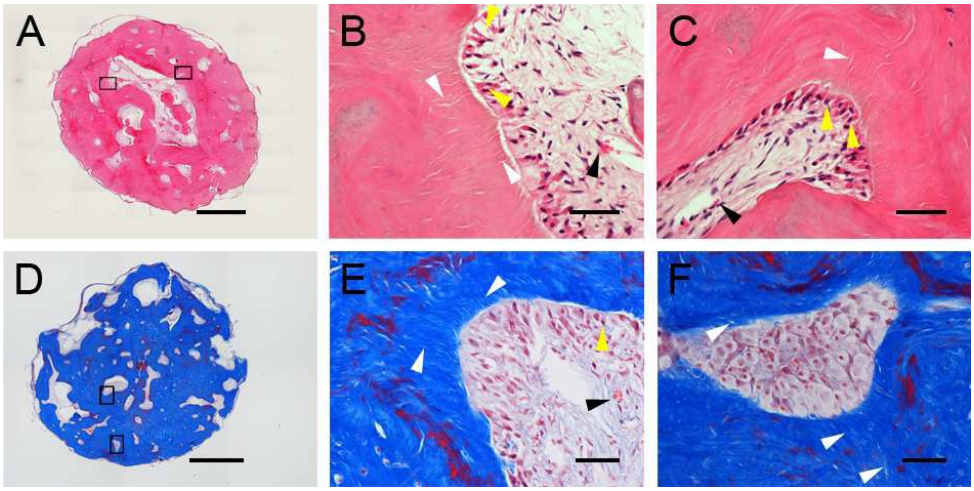

Figure 5

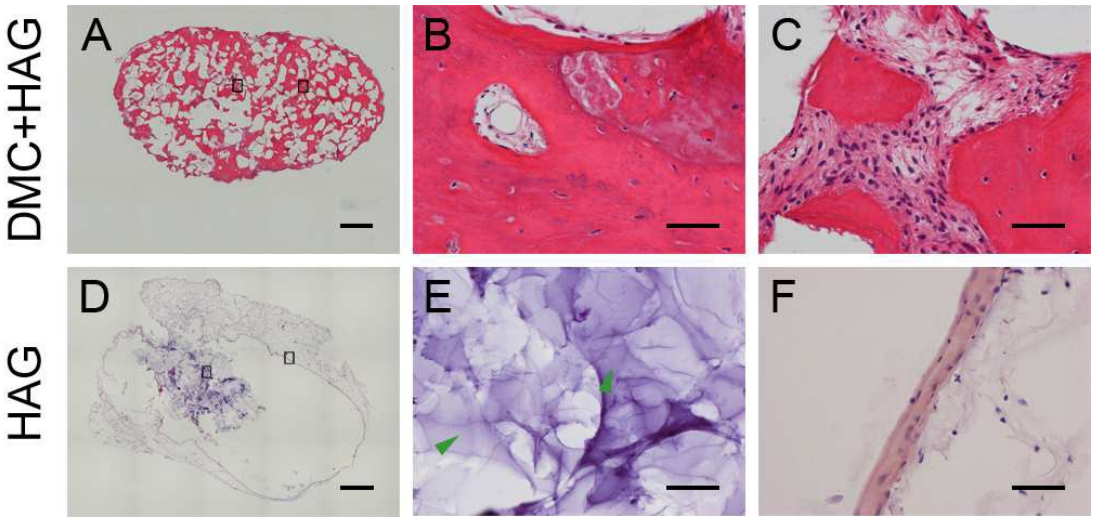

Figure 6

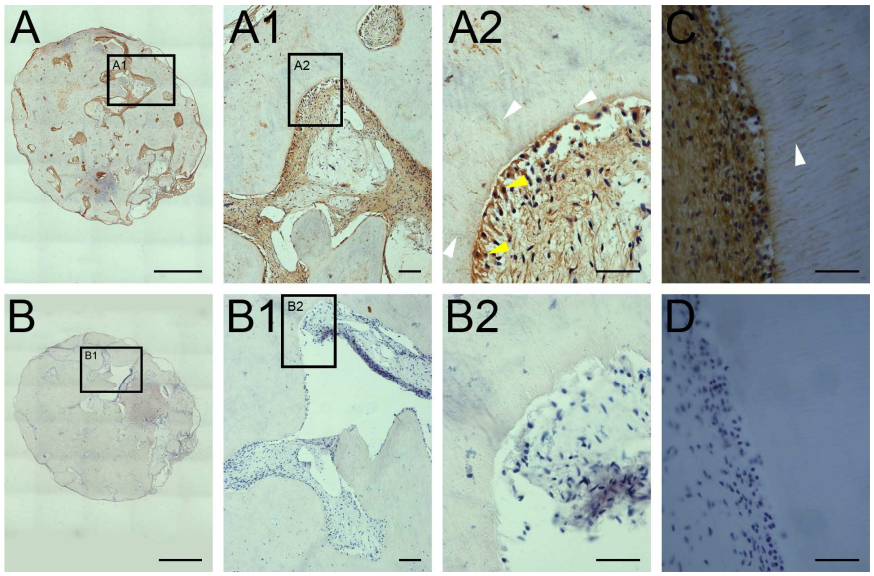

Figure 7

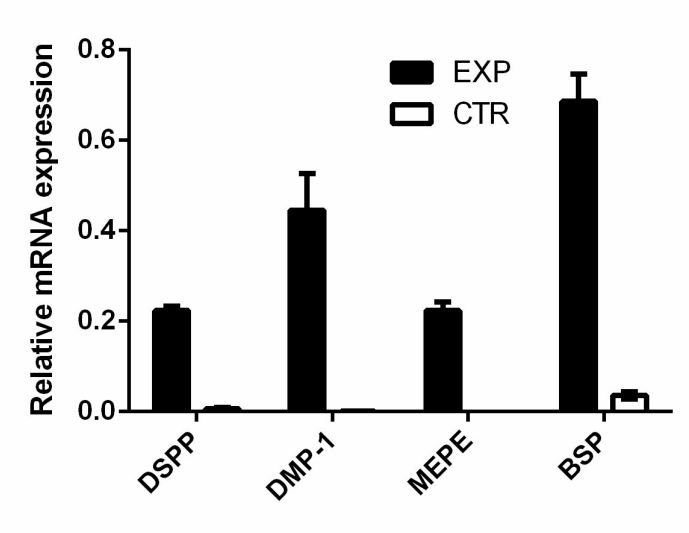

Figure 8

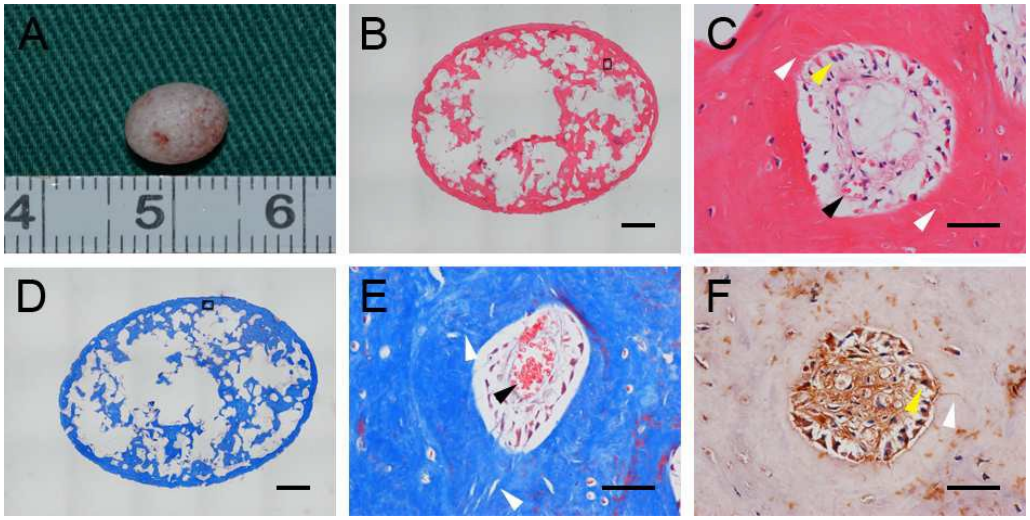

Figure 9

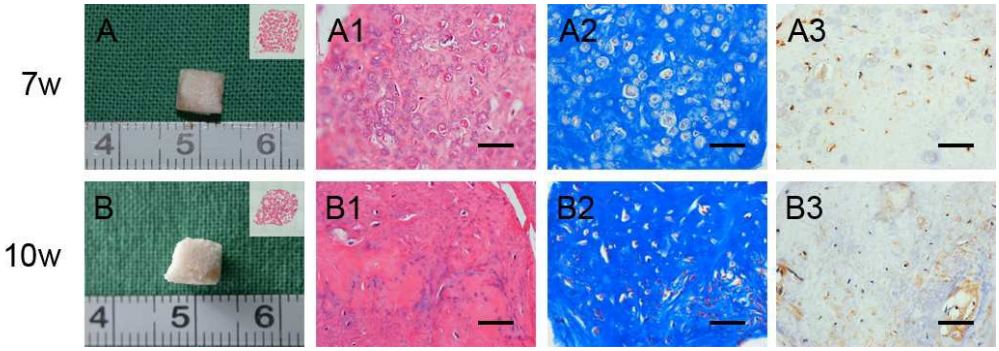

Figure 10

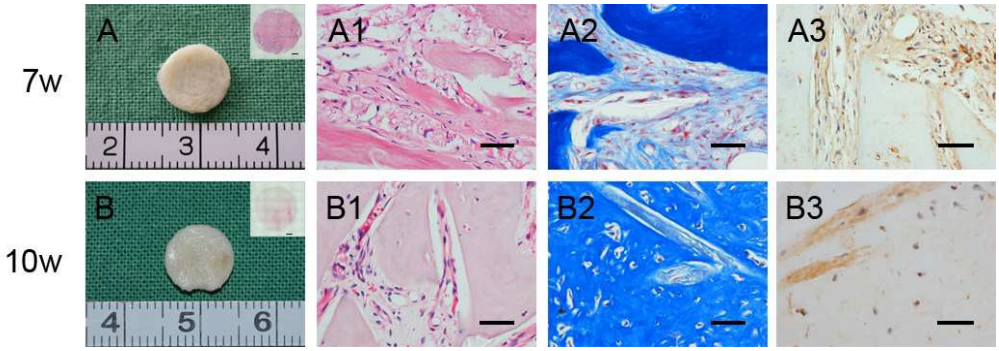

Figure 11

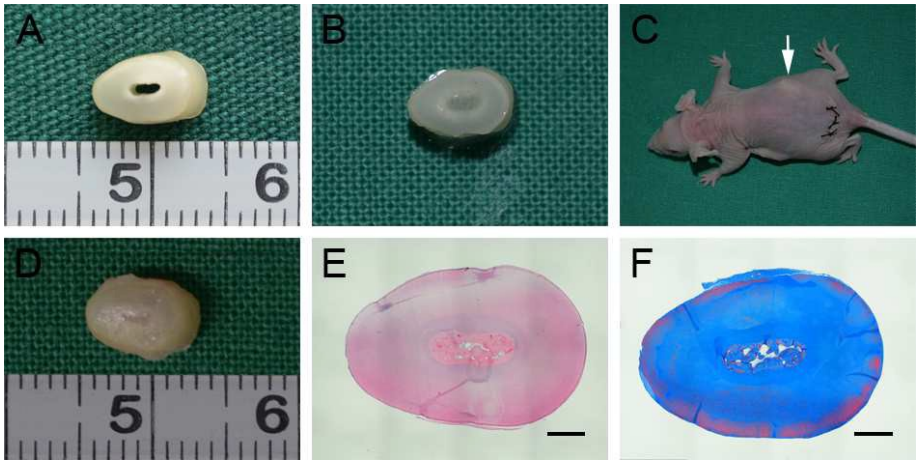

Figure 12

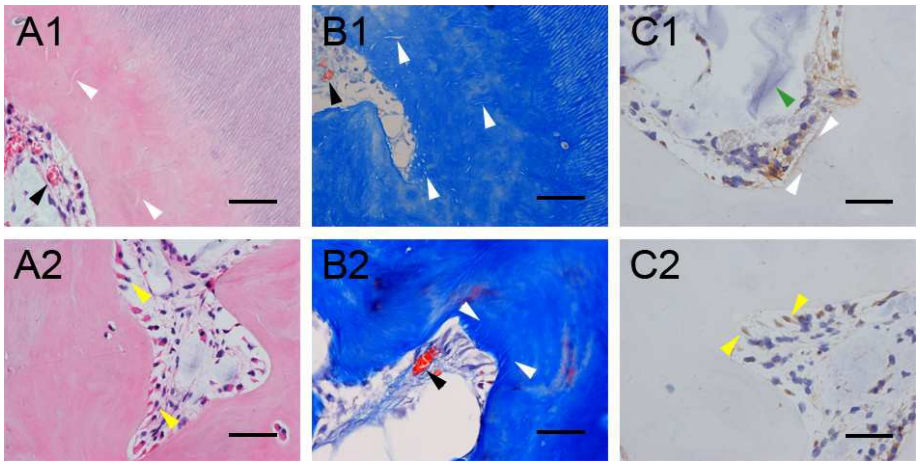

Figure 13

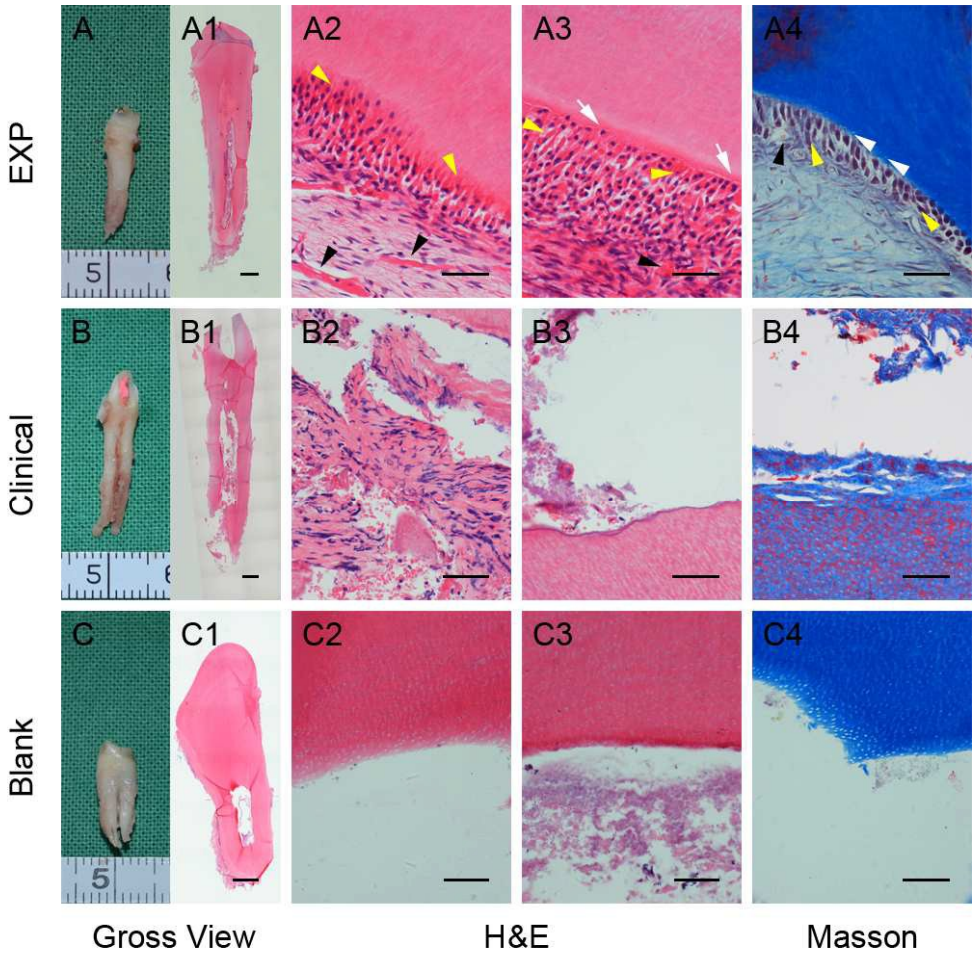

Figure 14

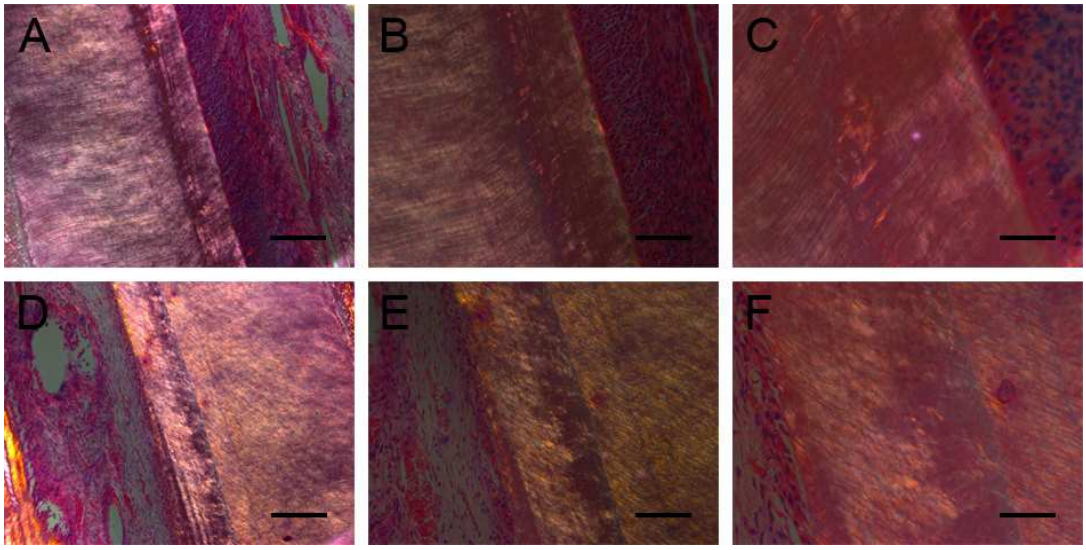

Figure 15

TOC

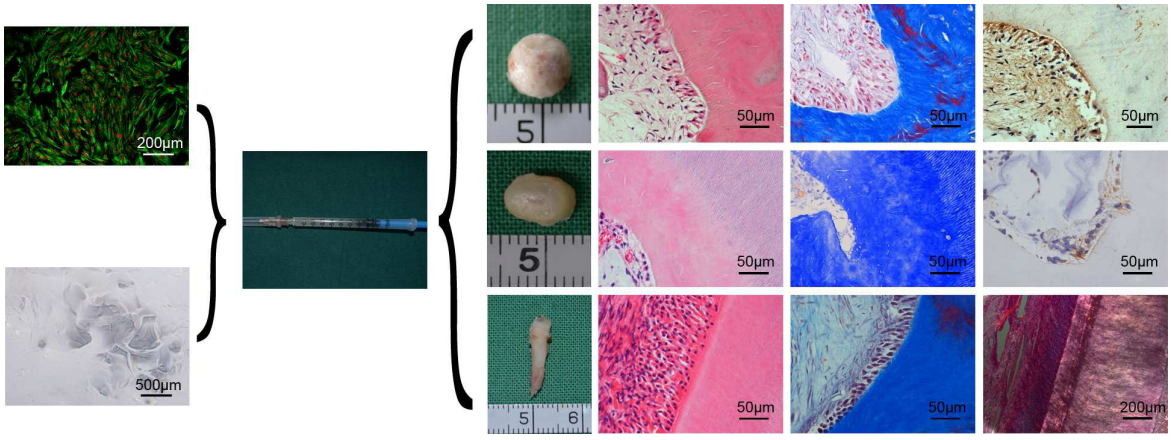

Injectable tissue engineering technique to regenerate dentin-pulp complex